Amino Acids (2012) 42:597–610
DOI 10.1007/s00726-011-1035-7

ORIGINAL ARTICLE

A combined model of hepatic polyamine and sulfur amino acid metabolism to analyze S-adenosyl methionine availability

Armando Reyes-Palomares · Raúl Montañez · Francisca Sánchez-Jiménez · Miguel Ángel Medina

Received: 8 February 2011 / Accepted: 26 March 2011 / Published online: 4 August 2011

Abstract Many molecular details remain to be uncovered concerning the regulation of polyamine metabolism. A previous model of mammalian polyamine metabolism showed that S-adenosyl methionine availability could play a key role in polyamine homeostasis. To get a deeper insight in this prediction, we have built a combined model by integration of the previously published polyamine model and one-carbon and glutathione metabolism model, published by different research groups. The combined model is robust and it is able to achieve physiological steady-state values, as well as to reproduce the predictions of the individual models. Furthermore, a transition between two versions of our model with new regulatory factors added properly simulates the switch in methionine adenosyl transferase isozymes occurring when the liver enters in proliferative conditions. The combined model is useful to support the previous prediction on the role of S-adenosyl methionine availability in polyamine homeostasis. Furthermore, it could be easily adapted to get deeper insights on the connections of polyamines with energy metabolism.

Keywords Metabolic modeling · Systems biology · Polyamines · S-adenosyl methionine · Methionine cycle · Folate cycle

The metabolites preceded by "b", "c" or "m" are located in the blood, the cytosol or mitochondria, respectively. Those metabolites without a precedent letter are locate in one compartment, or in the case of folate, formaldehyde, sarcosine, dimethylglycine can be included in different cellular compartments with the same concentration as a consequences of diffusion transport processes. The reactions are preceded by "V".

Electronic supplementary material The online version of this article (doi:10.1007/s00726-011-1035-7) contains supplementary material, which is available to authorized users.

A. Reyes-Palomares · R. Montañez · F. Sánchez-Jiménez · M. Á. Medina (✉)
Department of Molecular Biology and Biochemistry, Faculty of Science, University of Málaga, 29071 Málaga, Spain
e-mail: medina@uma.es

A. Reyes-Palomares · F. Sánchez-Jiménez · M. Á. Medina
Unit 741, CIBER de Enfermedades Raras (CIBERER), ISCIII, Málaga, Spain

Present Address:
R. Montañez
Institut de Biologia Evolutiva (CSIC-UPF), Passeig Marıtim de la Barceloneta 37-49, 08003 Barcelona, Spain

Introduction

Mammalian polyamine metabolism consists of a bi-cycle with two required entrances, ornithine and S-adenosyl methionine (SAM), and several alternative exits (Medina et al. 2003). The relevant regulatory roles of the short half-life enzymes ornithine decarboxylase (ODC), S-adenosylmethionine decarboxylase (SAMDC) (Berntsson et al. 1999) and spermidine/spermine acetyl transferase (SSAT) (Parry et al. 1995) are well documented. With a solid background in the study of polyamine metabolism regulation (among others, see Paz et al. 2001; Melgarejo et al. 2010), our group has previously claimed for more systemic approaches by using both omics technology and biocomputational models (among others, see Medina et al. 2005; Chaves et al. 2007; Montañez et al. 2007; Sánchez-Jiménez et al. 2007). In 2006, our group made public the first mathematical model of mammalian polyamine metabolism (Rodríguez-Caso et al. 2006). This model captured the tendencies observed for these key enzymes both in transgenic mice and in pharmacological intervention

experiments, i.e., MGBG (methylglyoxal bis(guanylhydrazone) (Marques et al. 2008; Agostinelli et al. 2010). Furthermore, the model unveiled (and explained in mathematic terms) the key regulatory role of SAM availability and acetyl-CoA/CoA recycling for polyamine regulation, two features which were not usually considered in systemic experimental studies concerning polyamine metabolism. Concerning acetyl-CoA availability, there were some previous experimental results pointing in the direction suggested by our model simulations (Kee et al. 2004), and evidence of the connection between polyamine metabolism and the oxidative metabolism (Pezzato et al. 2009). Shortly, after the publication of our model, new experimental data from independent group confirmed our predictions (Jell et al. 2007; Kramer et al. 2008). On the contrary, there were no available experimental data to test our suggestion that the branch of SAM production in the methyl cycle pathway could be relevant for polyamine homeostasis.

SAM is a main donor of methyl groups connecting polyamine, histamine, sulfur amino acid and folate metabolic pathways (Grillo and Colombatto 2008; Lu 2000) across 21 reactions in the KEGG human metabolic pathway. Therefore, SAM could be considered as a metabolic hub within the metabolite-reaction network (Montañez et al. 2010). Previous studies have proposed SAM as a physiological marker for hepatocytes and as a key element in their metabolic regulation (Finkelstein and Martin 1984; Mato et al. 2002; Prudova et al. 2006; Santamaría et al. 2006). The biosynthesis of SAM occurs in all mammalian cells in a reaction catalyzed by methionine adenosyltransferase (MAT). Two genes (*mat 1a* and *mat 2a*) encode for this essential enzyme; *mat 1a* is expressed mainly in the liver, whereas *mat2a* is widely distributed. The *mat2a* expression is induced in liver during the periods of rapid growth and dedifferentiation (Lu 2000). Both genes encode for two homologous MAT catalytic subunits, $\alpha 1$ and $\alpha 2$, respectively. The $\alpha 1$ subunits associated with different quaternary structure give rise to MAT-I/MAT-III isozymes. On the other hand, the $\alpha 2$ subunit can bind a regulatory β subunit (forming MAT-II isozyme) that confers the capability to be inhibited by the product SAM. Thus, although MAT isozymes catalyze the same reaction, they differ in kinetic and regulatory properties (Sullivan and Hoffman 1983). It has been shown that SAM availability decreases in response to a switch in the gene expression of different methionine adenosyltransferase (MAT) isozymes (Cai et al. 1998; Martínez-Chantar et al. 2002). Other experimental works have modeled the sulfur amino acid metabolism, but ignoring the flux distribution, driving to wrong interpretations based on correlations of metabolites levels and enzyme activities (Stipanuk and Dominy 2006). In this sense, a dynamical approach of this metabolic system can be very useful. Although several previous biocomputational works have modeled the methyl cycle, the sulfur metabolism and the MAT switch (Martinov et al. 2000; Reed et al. 2004; Nijhout et al. 2004; Prudova et al. 2005; Nijhout et al. 2006; Korendyaseva et al. 2008; Reed et al. 2008; Martinov et al. 2010), none of them has taken into account the regulatory role of the connection with polyamine metabolism. In order to bridge this gap, we decided to build a combined model.

This communication describes our detailed model of hepatic polyamine, methyl cycle and sulfur amino acid metabolism, and how this combined model can provide new insights on the role of SAM availability on polyamine homeostasis and on the pathophysiological implications of the MAT switch.

Materials and methods

Buidling of the first and second versions of the combined model

To build the combined model, we started by translating our original polyamine model written in Perl (Rodríguez-Caso et al. 2006) to compatible SBML (Hucka et al. 2003). A curated version of this model is currently available in BioModel database (Li et al. 2010; reference BIOMD 0000000190). We decided to combine this curated polyamine model with the curated one-carbon and glutathione metabolism model (reference BIOMD 0000000268), corresponding to that published by Reed and co-workers (Reed et al. 2008). The SBML file of the version 1 (first version) of our combined model is provided as Online Resource 1. To overcome the overlap of the MAT-I/-III reaction included in the glutathione model (Reed et al. 2008) with the MAT reaction included in our original polyamine model (Rodríguez-Caso et al. 2006), only the rate equations of glutathione model (Reed et al. 2008) taking into account the SAM biosynthesis through both isoenzymes separately were included in our combined model. Figure 1 shows our combined model depicted by making use of SBGN (Le Novère et al. 2009) graphical notation with the CellDesigner (http://www.celldesigner.org/). To simulate the MAT switch, we built a version 2 of our combined model, as it is provided in Online Resource 2. In this version, we included the MAT-II rate equation (Online Resource 3) in agreement with the kinetics described previously (Prudova et al. 2005; Sullivan and Hoffman 1983) and the V_{max} parameters for MAT-I/-III (Vm_MAT1 and Vm_MAT3, respectively) were fixed at zero ($\mu mol\ h^{-1}$) as it occurs in the MAT switch (Martínez-Chantar et al. 2002). Additionally, a regulation factor (Online Resource 3) was implemented in V_{max} parameters

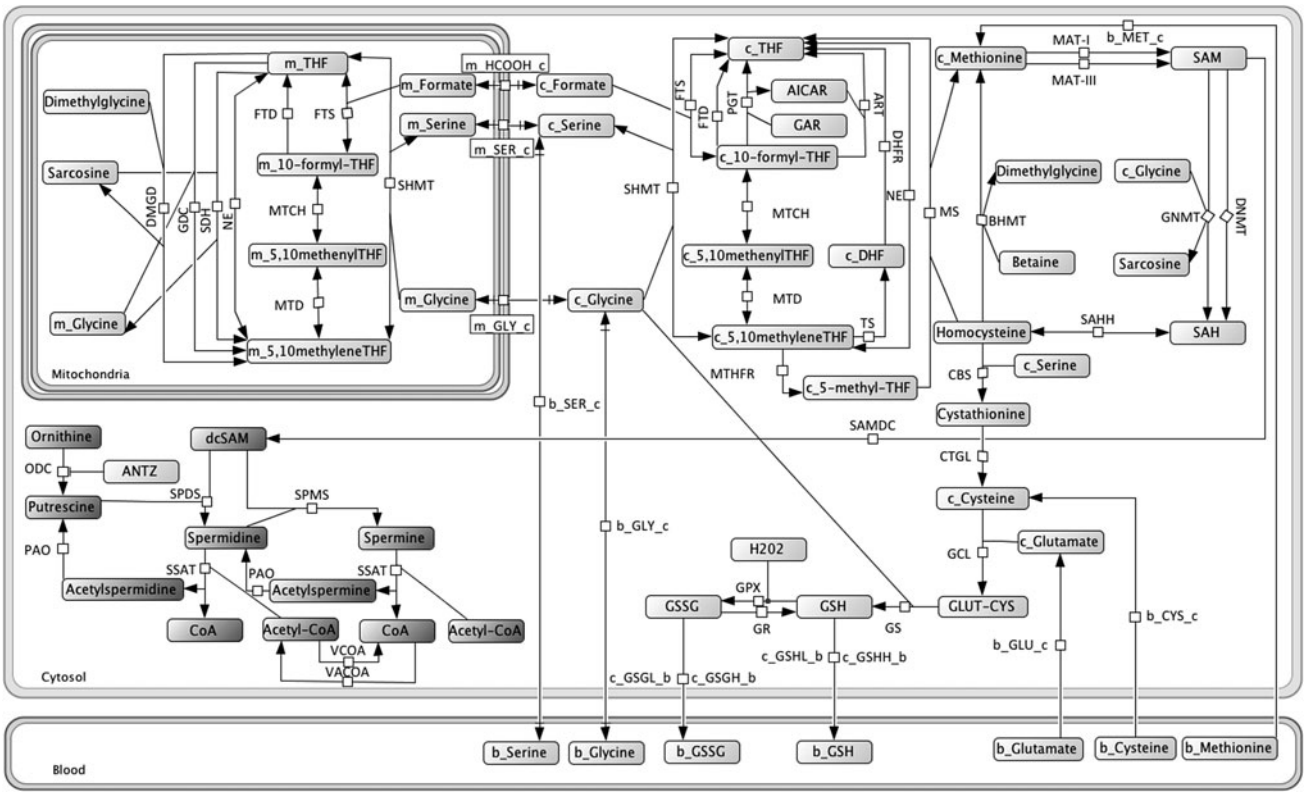

Fig. 1 Combined model of polyamines, one-carbon and glutathione metabolism (version 1). The main metabolites and biochemical reactions involved in polyamine (*dark gray*), folates, methionine and glutathione metabolism (*gray*) are depicted. This representation follows the specifications of the Systems Biology Graphical Notation (SBGN, www.sbgn.org). SAM (in the *upper right corner* with the *largest font*) represents the main connection between one-carbon metabolism plus transulfuration pathways and polyamine metabolism. The metabolites preceded by "b", "c" or "m" are located in the blood, the cytosol and mitochondria, respectively. Those metabolites without a precedent letter are located in one compartment only, or in the case of folate, formaldehyde, sarcosine and dimethylglycine can be included in different cellular compartments with the same concentration as a consequence of diffusion transport processes

for ODC and SAMDC to test the effects of the availability of SAM on the polyamine metabolism as a consequence of the switch in the MATs reactions. A similar approach were carried out in previous models (Prudova et al. 2005), but the biosynthetic reactions and catabolic mechanism were oversimplified.

Finally, the concentration of hydrogen peroxide was increased by 50% (from 0.01 to 0.015 μM) to include the effect of increased ROS in conditions of liver injury as in partial hepatectomy, hepatoma, and hepatocellular carcinoma (Huang et al. 2001), as well as a consequence of increased polyamine oxidation (Agostinelli et al. 2004).

Our models were designed under the theoretical framework of classical enzymology (taking into account our previous experience) and mathematically described as ordinary differential equation (ODEs) systems, containing affinity, inhibition and activation constants, specific activities and/or maximal velocities as their parameters. To evaluate the kinetic data used, we made use of the Systems Biology Metabolic Model (SBMM) assistant (Reyes-Palomares et al. 2009).The whole set of equations are provided in Online Resource 3, which includes the modified equations to build version 2 of the combined model. The initial values for parameters, reactions and metabolites in the model are provided in Online Resource 4 (Tables S1, S2) and Table 1, respectively. Models were simulated by using COPASI (Mendes et al. 2009).

Steady-state analysis

The steady-state analysis uses a deterministic ODE solver (LSODA) (Mendes et al. 2009). To run this analysis, the value of the "Aminoacid_input" parameter was fixed to one, considering constant the daily intake of amino acids from meals because perturbations generated for this parameter are very stiff and generate numerical instability. In addition, a kinetic stability analysis was performed in COPASI (Mendes et al. 2009) based on the linear stability analysis of the eigenvalues in the Jacobian matrix only valid for steady states. To perform the steady-state in the stability analysis for the forward and backward integration of the version 1 of the combined model, we modified default values of resolution parameter, referent to concentration variability along the time, from 10^{-9} to 10^{-6}, due to the stiffness of the model.

Table 1 List of metabolites used in the combined mode

Name	Compound	Type	Initial concentration (μM)	Steady-state concentration (μM)
1-(5′-Phosphoribosyl)-5-amino-4-imidazolecarboxamide	AICAR	Reactions	0.94	0.94
10-Formyltetrahydrofolate	c_10-formyl-THF	Reactions	3.41	3.26
10-Formyltetrahydrofolate	m_10-formyl-THF	Reactions	15.91	15.99
5-Methyltetrahydrofolate	c_5-methyl-THF	Reactions	4.50	5.36
5,10-Methenyltetrahydrofolate	c_5-10-methenyl-THF	Reactions	0.28	0.26
5,10-Methenyltetrahydrofolate	m_5-10-methenyl-THF	Reactions	1.55	1.55
5,10-Methylenetetrahydrofolate	c_5-10-methylene-THF	Reactions	0.51	0.46
5,10-Methylenetetrahydrofolate	m_5-10-methylene-THF	Reactions	1.67	1.67
5′-Phosphoribosylglycinamide	GAR	Fixed	10.00	10.00
Acetyl-CoA	Acetyl-CoA	Reactions	39.50	38.83
Betaine	Betaine	fixed	50.00	50.00
CO_2	CO_2	Fixed	0.00	0.00
CoA	CoA	Reactions	160.00	160.67
Cystathionine	Cystathionine	Reactions	36.88	32.30
Cysteine	b_Cysteine	Reactions	185.50	183.10
Cysteine	c_Cysteine	Reactions	194.97	179.79
Dihydrofolate	c_DHF	Reactions	0.04	0.04
DL-Glutamate	b_Glutamate	Reactions	60.43	60.47
DL-Glutamate	c_Glutamate	Reactions	3,219.40	3,236.78
DL-Serine	b_Serine	Assignment	150.00	150.00
DL-Serine	c_Serine	Reactions	562.83	571.23
DL-Serine	m_Serine	Reactions	2,114.87	2,150.06
dUMP	dUMP	Fixed	20.00	20.00
Folate	Folate[a]	Fixed	20.10	20.10
Formaldehyde	Formaldehyde[a]	Fixed	500.00	500.00
Formate	c_Formate	Reactions	13.09	13.98
Formate	m_Formate	Reactions	55.82	58.37
Gamma-L-Glutamyl-L-cysteine	Glutamyl-Cysteine	Reactions	9.81	9.61
Glutathione	b_GSH	Reactions	12.70	12.55
Glutathione	c_GSH	Reactions	6,590.85	6,272.51
Glutathione disulfide	b_GSSG	Reactions	0.48	0.47
Glutathione disulfide	c_GSSG	Reactions	61.30	59.81
Glycine	b_Glycine	Reactions	221.10	218.73
Glycine	c_Glycine	Reactions	924.43	927.56
Glycine	m_Glycine	Reactions	2,040.43	2,043.47
H_2O_2	H_2O_2	Fixed	0.01	0.01
Homocysteine	Homocysteine	Reactions	1.12	1.02
L-Ornithine	Ornithine	Fixed	300.00	300.00
Methionine	b_Methionine	Assignment	30.00	30.00
Methionine	c_Methionine	Reactions	49.19	50.60
N,*N*-Dimethylglycine	Dimethylglycine[a]	Reactions	0.71	0.68
*N*1-Acetylspermidine	Acetylspermidine	Reactions	0.01	0.90
*N*1-Acetylspermine	Acetylspermine	Reactions	0.01	0.03
NADPH	NADPH	Fixed	50.00	50.00
Putrescine	Putrescine	Reactions	0.01	98.20
S-Adenosyl-L-homocysteine	SAH	Reactions	19.14	15.56

Table 1 continued

Name	Compound	Type	Initial concentration (μM)	Steady-state concentration (μM)
S-Adenosyl-L-methionine	SAM	Reactions	81.17/**0.01**	65.06
S-Adenosylmethioninamine	dcSAM	Reactions	0.01	0.01
Sarcosine	Sarcosine[a]	Reactions	9.16	8.25
Spermidine	Spermidine	Reactions	0.01	79.59
Spermine	Spermine	Reactions	0.01	61.36
Tetrahydrofolate	c_THF	Reactions	4.67	4.03
Tetrahydrofolate	m_THF	Reactions	21.08	20.99

Initial and steady-state concentration values are provided

Names correspond to the nomenclature used in KEGG (http://www.genome.jp/kegg/) for biochemical compounds. Compounds match with the nomenclature used in Fig. 1: the compounds preceded by "b", "c" or "m" means they are in blood, cytosol and mitochondria compartments, respectively. *Type column* indicates the mathematical role of the compound in the combined model: *reactions* refer to compounds that are time-dependent parameters and their dynamical response is constrained by their related reactions and *fixed* refers to those compounds considered as time-independent parameters. SAM presents two different initial state concentrations, in *bold* that derived from Rodríguez-Caso et al. 2006

[a] Compounds that can diffuse between different compartments

Sensitivity analysis

Sensitivity analysis was carried out in COPASI by numerical differentiation using finite differences. In this analysis, all time-dependent parameters were differentiated with respect to all time-independent parameters of the combined model. The finite differences for numerical differentiation are calculated as the product of the current value of the time-independent parameters and a Delta factor (10^{-6}). If the resulting value is $<10^{-12}$ it is discarded and the 10^{-12} is used instead. This analysis generate a two dimensional matrix (Online Resource 5).

Time-course simulations and in silico experiments

In both versions of the model, time-course simulations were carried out to assess the progress of metabolites concentrations and reaction fluxes until reaching a stable value. To test the predictive power of the model, different perturbations were simulated following the same steps as described in the original models (Rodríguez-Caso et al. 2006; Reed et al. 2008). These in silico experiment used steady-state values as initial conditions.

Results

The combined model achieves steady-state values similar to those attained by the original models

Tables S2 (contained in Online Resource 4) and Table 1 show the steady-state flux and concentration values obtained in the simulation of the first version of the combined model for reactions and metabolites, respectively. These steady-state values are equal or very similar to those reported to be obtained in the simulations of the original models and are attained at the same physiological times (Rodríguez-Caso et al. 2006; Reed et al. 2008). It is noteworthy also how the combined model keeps the metabolite fluctuations within the physiological rank, in the time needed to achieve the steady state.

The combined model is robust

The kinetic stability analysis showed an asymptotically stable state presenting transient states in its vicinity with oscillatory components. An exhaustive sensitivity analysis (provided as Online Resource 5) indicates that the combined model is essentially robust, in spite of the fact of having been built from two independent kinetic models that were designed according to very different principles.

The combined model reproduces the predictions attained by the original models

Figures 2 and 3 show that our combined model faithfully reproduces the main predictions obtained with simulations from the original models (Rodríguez-Caso et al. 2006; Reed et al. 2008). Concerning the polyamine metabolism, Fig. 2 reproduces both experimental data and the original polyamine model simulations related to the modulation of the three key control enzymes in polyamine metabolism. Concretely, we analyzed the effects of treatments with DFMO (an inhibitor of ODC), MGBG (an inhibitor of SAMDC) and DENSPM (a "superinducer" of SSAT), as well as the effects of the bioavailability of acetyl-CoA as a function of its recycling. On the other hand,

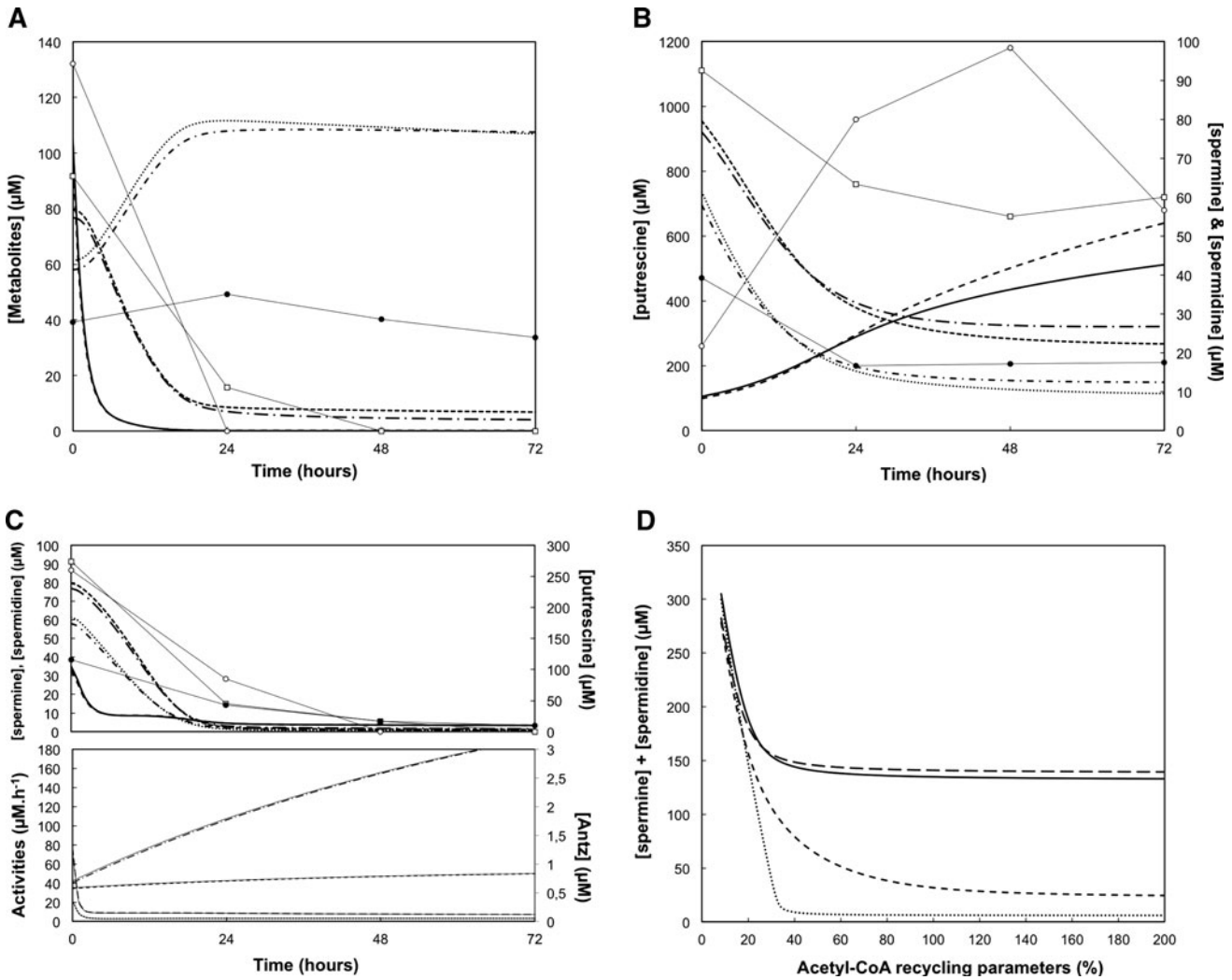

Fig. 2 In silico experiments with the combined model (version 1) reproduces the predictions of the original mammalian polyamine metabolism model (Rodríguez-Caso et al. 2006). **a** DFMO (an irreversible inhibitor of ODC) effects on polyamine levels in both time-course simulations (isolated and combined models) and experiments data from (Korhonen et al. 2001). For the original model of polyamines, in silico simulations are shown as follows: putrescine (*continuous line*), spermidine (*segment and dotted line*), and spermine (*dashed and dotted line*). For the combined model, in silico simulations are shown as follows: putrescine (*segment line*), spermidine (*dashed line*), and spermine (*dotted line*). Experimental data are shown as follows: putrescine (*empty circles*), spermidine (*empty squares*), and spermine (*full circles*). **b** MGBG (a potent competitive inhibitor of SAMDC) effects on polyamine levels in both time-course simulations (original and combined models) and experiments data from (Korhonen et al. 2001). *Lines* as in (**a**). **c** DENSPM (a very potent inducer of SSAT) effects on polyamine levels (*up*) and short lived enzymes (*down*). For polyamines, we used *lines* as in (**a**). For enzymes: ODC (*continuous line*), Antz (*dashed line*), SAMdc (*dotted line*), and SSAT (*segment and dotted line*). Each *line* is accompanied by a very *thin line* attached that corresponds to the results of the simulation carried out in the combined model. **d** Effects of acetyl-CoA recycling rate in the free polyamine levels once steady state is reached. In the model of polyamines, basal conditions (*continuous line*); tenfold induced SSAT activity conditions (*dotted line*). In the combined model, basal conditions (*segment line*); tenfold induced SSAT activity conditions (*dashed line*). For the cases of induction of SSAT, we considered SSAT activity to be a time-independent parameter

Fig. 3 reproduces responses to amino acid input through dietary intake, as well as the cyclic perturbations that introduce in certain metabolite concentrations and fluxes. These predictions are well supported by experimental observations (Rodríguez-Caso et al. 2006; Reed et al. 2008 and references mentioned therein). Other simulations carried out in the original descriptions of the individual models were also faithfully reproduced by our combined model (results not shown).

A transition from version 1 to version 2 of our combined model is necessary to reproduce the metabolic consequences of a MAT-I/-III to MAT-II switch

As mentioned earlier, it is well documented that under proliferative circumstances there is a switch from MAT-I/-III to MAT-II activity in the mammalian liver. Since the

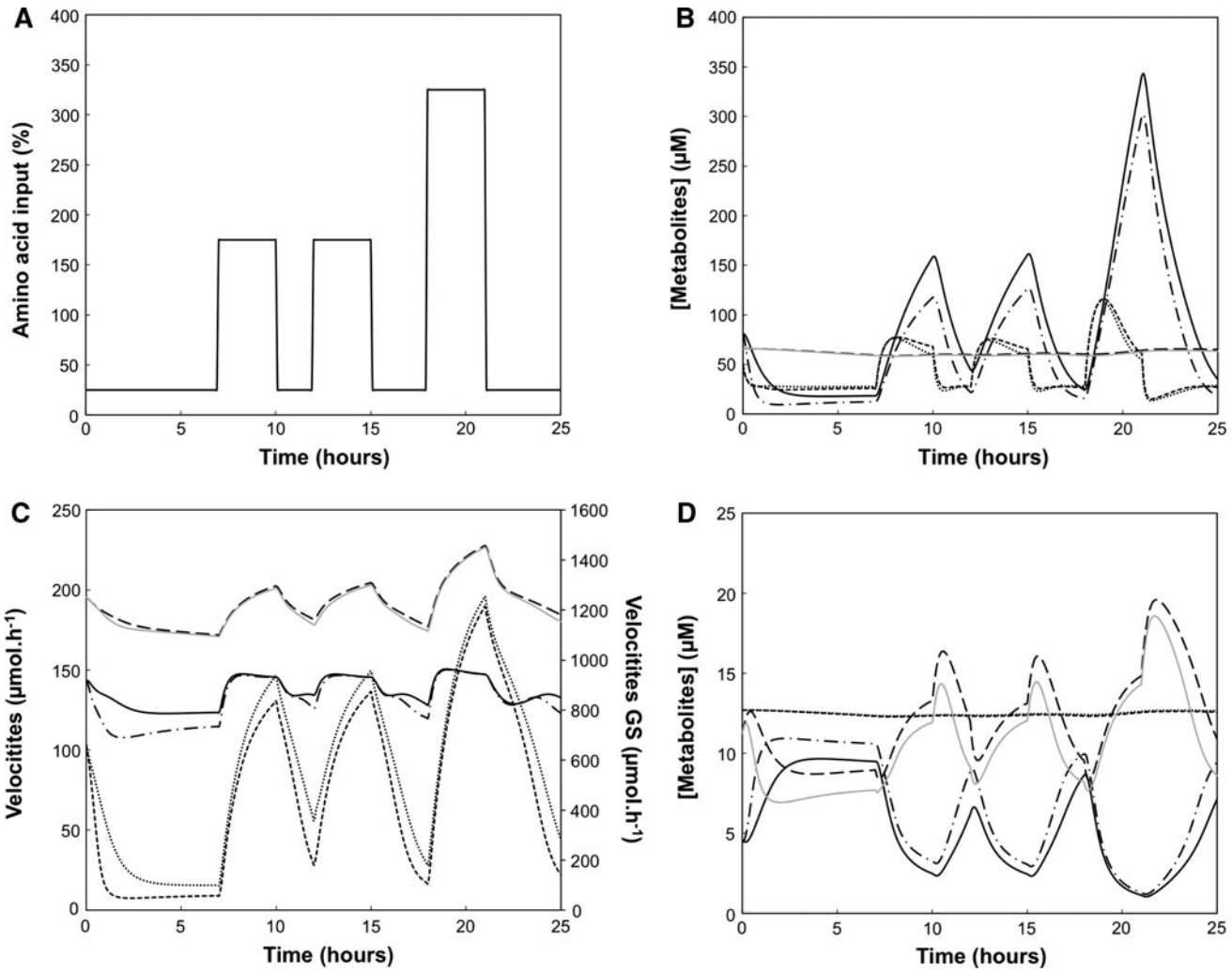

Fig. 3 In silico experiments with the combined model (version 1) reproduces the predictions of the original one-carbon and glutathione metabolism model (Reed et al. 2008). **a** Time-course of the amino acid input to the hepatocyte in the models throughout a day. **b** Time-course simulations of the changes in concentrations of SAM, c_methionine and c_GSH. For the original the glutathione model: SAM (*continuous line*), c_methionine (*dotted line*) and 100 times increased cGSH (*segment line*). For the combined model: SAM (*segment and dotted line*), c_methionine (*dashed line*) and 100 times increased cGSH (*gray line*) for the representation. **c** Time-course simulations of the changes in the fluxes of V_DNMT, V_CBS and V_GS. In the glutathione model: V_DNMT (*continuous line*), V_CBS (*dotted line*) and V_GS (*segment line*). In the combined model: V_DNMT (*segment and dotted line*), V_CBS (*dashed line*) and V_GS (*gray line*). **d** Time-course simulations of the changes in the concentrations of c_5-methyl-THF, b_GSH and homocysteine. In the glutathione model: c_5-methyl-THF (*continuous line*), b_GSH (*dotted line*) and ten times increased homocysteine (*segment line*). In the combined model: c_5-methyl-THF (*segment and dotted line*),b_GSH (*dashed line*) and ten times increased homocysteine (*gray line*)

curated one-carbon and glutathione metabolism model (BIOMD 0000000268) integrated in our combined model included equations for MAT-I/-III, but not for MAT-II, we decided to build another version of our model by setting the parameters (V_{max}) corresponding to MAT-I/-III to zero and including the MAT-II velocity reaction (Online Resource 3). Thus, a transition from version 1 to version 2 of our combined model should allow us to simulate the switch that has been reported to regulate the liver function (Mato et al. 2002). However, as shown by Fig. 4, the simple exchange of MAT-I/-III to MAT-II kinetic data in our initial integrated model is not enough to properly simulate the metabolic MAT switch consequences observed experimentally; therefore, other factors should be taken into account and some adjustments were necessary to improve the predictive capabilities of our model. Current knowledge allows us to infer the importance of the regulatory role of SAM on this switch and the homeostasis of liver metabolism (Finkelstein et al. 1975; Finkelstein and Martin 1984; Mato et al. 2002; Prudova et al. 2006), which seems to

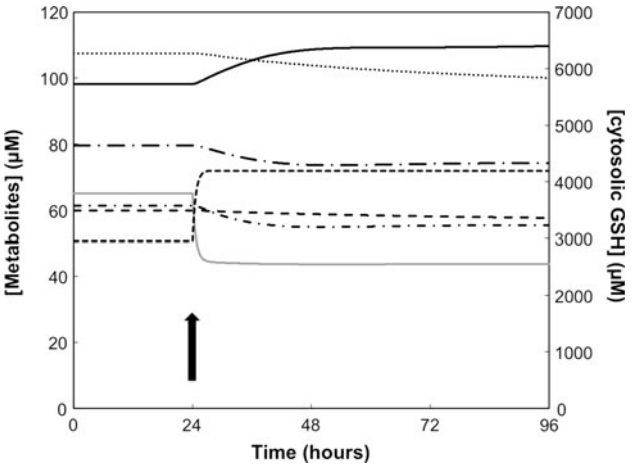

Fig. 4 Time-course simulation (96 h) of the MAT isozyme expression switch (at time 24 h, as indicated by the *arrow*, MAT-I/-III are switched off and MAT-II is switched in) effects on concentration of major regulated metabolites. SAM (*gray line*), putrescine (*continuous line*), c_GSSG (*segment line*), spermidine (*segment and dotted line*), spermine (*dashed-dotted line*), c_methionine (*dashed line*), c_GSH (*dotted line*)

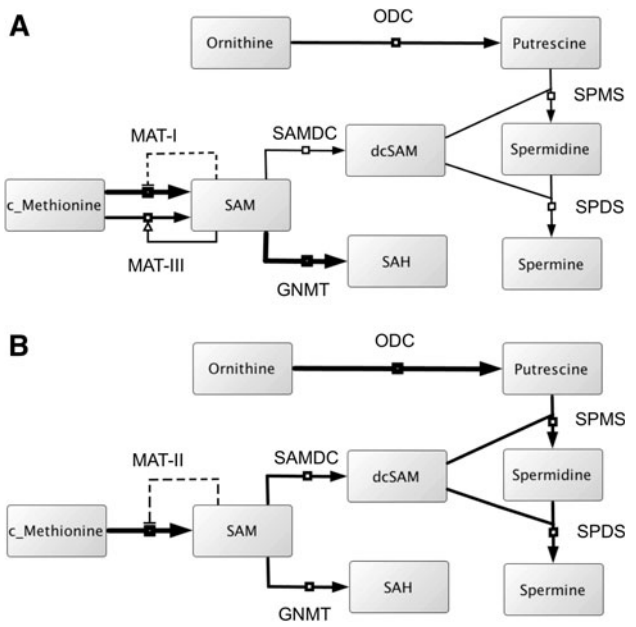

Fig. 5 Schematic representation of the switch in the expresion of methionine adenosyltransferase (EC 2.5.1.6) coding genes and fluxes through reactions of polyamine biosynthesis. Hepatocyte proliferation is related to the inactivation of the activity and expression of MAT-I and -III, as well as to the increased activity of MAT-II. **a** MAT-I/MAT-III regulation by SAM in the version 1 of the combined metabolic model. **b** MAT-II regulation by SAM in the hepatocyte proliferating model (version 2, see methods and text). The thickness of the reactions (*arrows*) is correlated with the flux value in each condition

involve polyamine metabolism. In fact, it is reported that an inverse correlation between SAM depletion and the activities of two key enzymes for polyamine synthesis

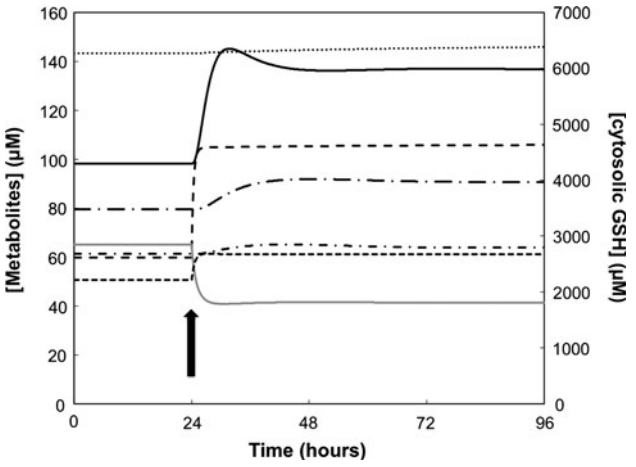

Fig. 6 Time-course simulation (96 h) of the MAT isozymic expression switch (at time 24 h, as indicated by the *arrow*, version 1 is substituted by version 2 of the combined model) effects on concentration of major regulated metabolites taking into account SAM regulation in polyamine biosynthetic enzymes ODC and SAMDC. *Lines* as in Fig. 4

ODC and SAMDC is due to uncharacterized mechanisms (Mikol and Poirier 1981; Kramer et al. 1987; Kramer et al. 1988). In addition, the overexpression of ODC in liver under different proliferative circumstances as in partial hepatectomy is well known (Russell and McVicker 1971; Kubo et al. 1998). Therefore, to simulate these changes, we introduced a SAM-dependent regulatory factor on both SAMDC and ODC V_{max} equations (see Online Resource 3) in the version 2 of our model due to the decreased SAM levels. Figure 5 depicts the fluxes distributions in polyamine metabolism associated with this MAT-I/-III (panel A) to MAT-II (panel B) switch, in agreement with a basal (version 1) and a proliferative (version 2) physiological condition, respectively. Furthermore, since proliferation has been associated with increased oxidative stress and as an effect of increased activity of polyamine oxidation (Agostinelli et al. 2004), we also increased by 50% the levels of hydrogen peroxide in the version 2 of our combined models. In response to increased oxidative stress, glutathione synthesis is increased and it leads to rise the cytosolic levels of glutathione, in agreement with experimental data (Vitvitsky et al. 2003, 2006). Figure 6 shows simulations of transitions from version 1 to version 2 of the combined model (this last one incorporating the previously mentioned changes). It should be underscored that under these conditions our models were able to simulate metabolic changes experimentally proven as the effects of SAM depletion on polyamine biosynthesis (Mikol and Poirier 1981; Kramer et al. 1987, 1988), polyamine metabolism in liver cancer (Russell and McVicker 1971; Williams-Ashman et al. 1972; Kubo et al. 1998) and increased

glutathione level in hepatocellular carcinoma (Huang et al. 2001).

Version 2 of the integrated model predicts experimental observation under different hepatic proliferative circumstances

Due to the high regenerative potential of liver, partial hepatectomy is a good experimental model to analyze metabolic changes associated with a transition to these regenerating conditions (Latasa et al. 2001; Huang et al. 1998). Figure 7 show that our combined model is able to simulate and properly predict some relevant features of polyamine metabolism under proliferative conditions (Russell and McVicker 1971).

Liver cancer, in correlation with a growing genetic instability in the carcinogenesis process, leads to metabolic responses similar to those ocurring in proliferating hepatocytes after a partial hepatectomy. According to all previous knowledge, liver cancer could be a good model to be tested in the version 2 of the combined model. Figure 8 compares the changes in polyamine concentrations and ODC activity obtained in MAT switch simulation in silico experiments with those observed experimentally under circumstances of hepatoma with different proliferation rates (Williams-Ashman et al. 1972) and hepatocellular

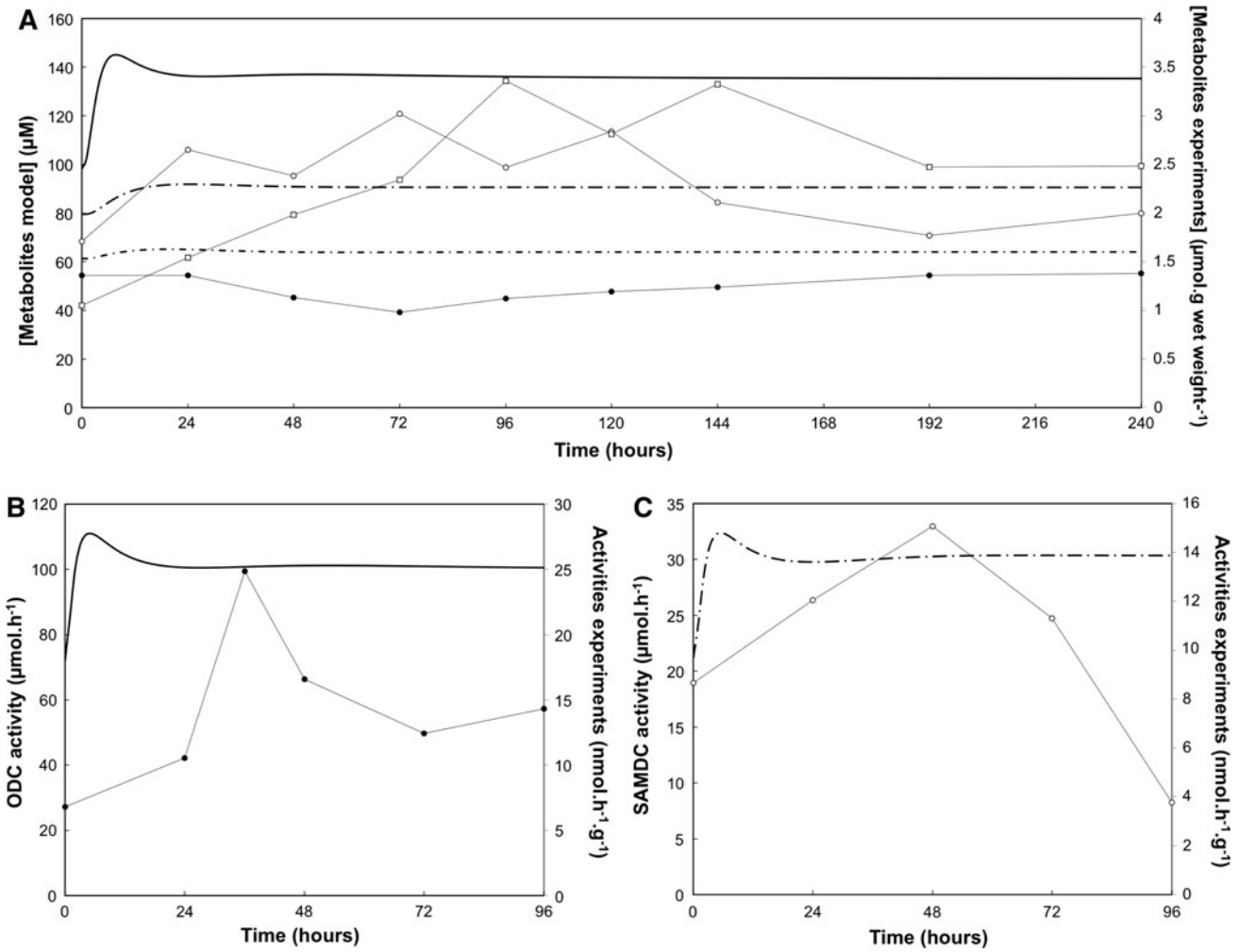

Fig. 7 Polyamine levels and polyamine biosynthetic activities in partial hepatectomy experiments (Russell and McVicker 1971) and in silico time-course simulation results of the MAT expression switch. **a** Polyamine levels. In silico experiments are shown as follows: putrescine (*continuous line*), spermidine (*segment and dotted line*), and spermine (*dashed and dotted line*). Experimental data are shown as follows: putrescine* (*empty circles*), spermidine (*empty squares*), and spermine (*full circles*). *Asterisk* indicates that putrescine experiments concentration values have been increased ten times for the representation. **b** ODC activity. In silico simulation data (*continuous line*); experimental data (*full circles*). **c** SAMDC activity. In silico simulation data (*segment and dotted line*); experimental data (*empty circles*)

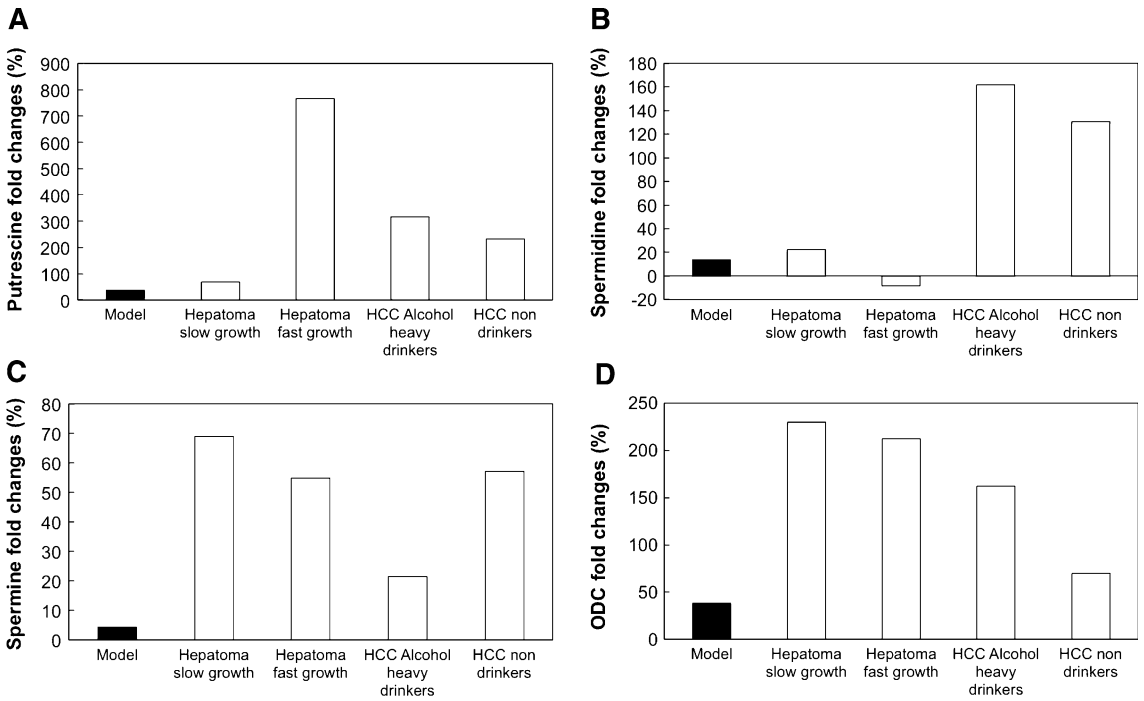

Fig. 8 Comparisons in both hepatic polyamine concentrations and ODC activity fold changes between in silico experiments results and different malignant models (hepatoma and hepatocellular carcinoma experimental data). *Black bars* indicate results from the version 1 of the model. For hepatoma experimental data (Williams-Ashman et al. 1972) the fold changes (%) mean values respect to the controls corresponding to slow/intermediate and fast cell growth groups are depicted. In hepatocellular carcinoma experimental data (Kubo et al. 1998), the fold changes mean values respect to the controls (corresponding to heavy alcohol consumers and moderate or non consumers) are depicted

carcinoma associated or not with effects of alcohol abuse (Kubo et al. 1998).

Discussion

Current utility of bottom-up approaches based on kinetic metabolic modeling

Since a few years ago, molecular systems biology approaches are feasible to build genome-scale metabolic network models (Chandrasekaran and Price 2010; Ma et al. 2007; Duarte et al. 2007), as well as genome-scale kinetic models of the whole cellular metabolism (Jamshidi and Palsson 2008; Smallbone et al. 2010). However, these approaches provide a low resolution, and therefore when higher degrees of details are required, classical detailed kinetic models based on accumulated kinetic and metabolic knowledge are still convenient and useful alternatives (Montañez et al. 2008; Curien et al. 2009; Raftos et al. 2010). Accepting that cellular functionality could be seamlessly partitioned into a collection of modules (Hartwell et al. 1999); Lauffenburger 2000; Shen-Orr et al. 2002) and that this modularity can be extended to the metabolism (Rao and Arkin 2001; Newman 2006), then a bottom-up modular integration approach seems an acceptable way to build bigger metabolic models from simpler, available ones. This bottom-up approach could lead to the effective building of the so-called silicon cell (Snoep et al. 2006).

In this study, we have used this bottom-up strategy to simply integrate two previously mathematical metabolic models (Rodríguez-Caso et al. 2006; Reed et al. 2008) into a combined model easily adaptable to simulate transitions to proliferative conditions in the liver. In the case of our original model of mammalian polyamine metabolism (Rodríguez-Caso et al. 2006), which was written in Perl, we decided to translate it into standard SBML. Curation of this adapted model allowed us to detect and restore some minor errors solved in its currently available Biomodels version (reference BIOMD 0000000190). Based on our experience with our own published model, we decided to use also the curated Biomodel version of the one-carbon and glutathione metabolism model (reference BIOMD 0000000268). It is noteworthy to mention that this model was in fact built by its authors from previously published models from their group by the aforementioned bottom-up strategy (Reed et al. 2004; Nijhout et al. 2004; Prudova et al. 2005; Nijhout et al. 2006; Korendyaseva et al. 2008; Reed et al. 2008).

Reliability and robustness of our combined model

It must be emphasized that the "philosophy" behind the way in which our group built the polyamine metabolism model and that applied by Reed et al. (2008) in the construction of their one-carbon and glutathione metabolism model are remarkably different. Whereas in this last model, the authors use physiological values of metabolites as initial concentration values, those not fixed values of metabolite concentrations considered in our polyamine metabolism model were assigned an initial value of 0.01 micromolar (very close to zero), as shown in Table 1. The conservative approach adopted by Reed et al. (2008) means that from the beginning they build a model that should be fit well to steady-state conditions, allowing only small changes in these initial values. Therefore, it should not be a surprise at all that steady-state concentration values are all very close to the selected initial values. We think that our approach is much stronger, since from initial conditions far away from actual physiological values, our model was able to reach completely physiological steady-state values (Rodríguez-Caso et al. 2006).

Modular reaction systems are more robust and converge to an equilibrium state faster than the less modular systems (Holme 2011). In this way, we were confident that these capabilities of metabolism to act as coordinated but relatively autonomous functional modules could allow us to successfully build integrated models by combining models of metabolic pathways as suggested by synthetic biology (Andrianantoandro et al. 2006). Models may come from different groups even in the case that the "philosophies" behind the way of building were clearly different, as it is the case of the two models integrated in our combined model. Therefore, we assumed all the assumptions of each individual model in our combined model (Fig. 1). Steady-state analysis of the version 1 of our combined model (Tables S2 contained in Online Resource 4 and 1) clearly shows the reliability of our model in capturing the main features of the original ones. Furthermore, sensitive analysis (Online Resource 5) indicates that the combined model is essentially robust and, in any case, as least as robust as the original models are.

The ability of our combined model to faithfully simulate steady-state conditions along with its proven robustness suggested that our model should also be able to properly simulate conditions of overexpression and/or inhibition of key enzymes for both individual previous models. This was the case, as undoubtedly shown in results depicted in Figs. 2 and 3.

Predictive potential of the present combined model

One unexpected prediction of our polyamine model was that SAM availability could have a relevant role in polyamine homeostasis (Rodríguez-Caso et al. 2006). SAM is a major donor of methyl groups for many methylation reactions and, at the same time, plays a relevant role in methyl cycle, sulfur amino acid metabolism, and as a precursor for both polyamines and histamine biosynthesis (Lu 2000; Medina et al. 2003, 2005). Therefore, we considered relevant and interesting to integrate the folate/methyl bi-cycle and sulfur amino acid metabolism into our original polyamine metabolism model to get further insights on the actual role of SAM availability in polyamine homeostasis. Since the one-carbon and glutathione metabolism model (Reed et al. 2008) contained more precise kinetic data concerning MAT-I/-III, as compared with our previous polyamine model (Rodríguez-Caso et al. 2006), which only considered MAT-I kinetics, in the version 1 of our combined model, we maintained MAT-I/-III as considered by the first individual model. In fact, MAT-I and MAT-III represent two different aggregation states (tetramer vs. dimer, respectively) of the same 395 amino acids α1 catalytic subunit encoded by the gene *mat1a* (Sánchez del Pino et al. 2002). However, there is a second *mat2a* gene encoding for 396 amino acids α2 catalytic subunit sharing 84% sequence identity with α1 subunit (Kotb et al. 1997). Whereas *mat2a* gene seems to be constitutively expressed in all mammalian tissues that have been examined (Mato et al. 2002), *mat1a* is only expressed in adult liver (Gil et al. 1996). This difference in the pattern of expression is interesting and it is related with the regulatory role assigned to SAM as a control switch that regulates essential hepatic functions such as liver regeneration and differentiation, as well as the sensitivity of this organ to injury (Corrales et al. 2002; Mato et al. 2002; Sánchez del Pino et al. 2002). In fact, it is well documented that high levels of SAM inhibit *mat2a* expression, as it is the case in the healthy adult liver. Under normal physiological conditions, two main mechanisms operate in the liver maintaining relatively high SAM concentrations: upregulation by SAM of *mat1a* expression and the high catalytic capacity of MAT-I/-III to convert dietary methionine into SAM. However, under conditions in which SAM availability is reduced (as it is the case of proliferative states demanding higher levels of methylation reactions), *mat2a* repression stops and MAT-II activity becomes a major source of SAM, which is not considered in the original individual models of polyamine and one-carbon and glutathione metabolism (Rodríguez-Caso et al. 2006; Reed et al. 2008). Therefore, to be able to properly simulate this metabolic switch, we decided to build a modified, version 2 of our combined model in which MAT-I/-III is substituted by MAT-II. On the other hand, it has been reported that the key regulatory enzyme in mammalian polyamine biosynthesis, ODC, behaves as a proto-oncogene with increased expression and activity under proliferative conditions

(Auvinen et al. 1992). Furthermore, proliferative conditions as well as injury could lead to oxidative stress, which in turn could contribute to inactivate MAT-I/-III and to reduce hepatic SAM levels. All these observed data could explain why a simple transition from version 1 to version 2 model was not enough to reproduce the real behavior of liver upon MAT-I/-III to MAT-II switch (Fig. 5). In fact, the incorporation of regulation by SAM of both ODC and SAMDC activities and a modest 50% increase in the fixed levels of hydrogen peroxide in the version 2 model was enough to solve this limitation (Fig. 6).

Proceeding further towards our final goal, the current knowledge of the MAT-I/-III to MAT-II switch allows us to predict important changes in the metabolic fluxes concerning polyamine biosynthesis as depicted in Fig. 6. Therefore, it could be expected from a metabolic model with actual predictive power that it could confirm the proposed role of SAM availability in polyamine homeostasis. This seems to be the case of our combined model, which in fact predicts an important impact of SAM availability on liver polyamine metabolism (Figs. 6, 7). Both SAM and polyamines are closely related metabolites that directly connect nitrogen metabolism with gene expression regulation. Our previous polyamine model predicts that Met/SAM availability could regulate polyamine metabolism in a positive way. However, the model ignored the existence of different MAT isozymes with different regulatory properties. When applied to hepatic-related biomedical problems, it was absolutely required to enrich the model with respect to MAT regulatory properties. In the case of a MAT-I/-III-MAT-II transition, SAM levels are reduced and it was necessary to introduce an inverse regulatory factor on ODC and SAMDC activities (proposed by previous bibliography) to properly reproduce the experimental observations obtained with hepatic proliferating models. In the case of hepatectomy, our model predicts reasonably well the impact of this situation on polyamine metabolism (Fig. 7). Furthermore, this also seems to be the case of hepatocarcinoma, a pathological situation that illustrates well the fact that *mat2a* gene expression is modulated as an adaptive response of the cell to methionine availability (Martínez-Chantar et al. 2003). In all the experimental cases (experimental rat hepatoma with slow and fast growth, and hepatocellular carcinoma in humans with and without previous alcohol abuse), it also reported a clear trend to increased levels of putrescine, spermidine and spermine and increased ODC activity (Williams-Ashman et al. 1972; Kubo et al. 1998), with the exception of a slight decrease reported for spermidine levels in fast growth hepatoma (Williams-Ashman et al. 1972). Our MAT switch simulations depicted in Fig. 8 could reproduce qualitatively the tendencies for polyamine concentrations and ODC activity found in experimental models. Nevertheless, a lack of information exists on the mechanisms for which decreased SAM levels induce polyamine synthesis enzymes. This could explain why our model can predict tendencies but the predicted perceptual changes are lower than the experimentally observed ones. This study reveals this SAM-dependent regulatory effect on polyamine metabolism as a key factor to understand SAM-polyamine relationship in the context of hepatic functions. Future experimental works are required to decipher these molecular mechanisms.

Concluding remarks

Our work illustrates the convenience of bottom-up approaches in kinetic metabolic models. The resulting versions of our combined model are robust and they recapitulate well the main features of the individual models used in their construction. Iterative contrast with experimental results and refining allow us to reveal the existence of newly important regulatory steps deserving further experimental development, to enrich our integrated model. Finally, the model is able to predict general tendencies under different physiopathological conditions in which SAM availability is affected. This model is also a further step to build future versions to get further information on the integration of these metabolic modules with the energy metabolism. The role of acetyl-CoA recycling on both polyamine metabolism and metabolic homeostasis in general deserves to be analyzed in the near future.

Acknowledgments Our experimental work is supported by grants PS09/02216, SAF2008-02522 and SAF2011-26518 (Spanish Ministry of Science and Innovation), and PIE P08-CTS-3759, CVI-6585 and funds from group BIO-267 (Andalusian Government). The "CIBER de Enfermedades Raras" is an initiative from the ISCIII (Spain). The funders had no role in study design, data collection and analysis, decision to publish, or preparation of the manuscript. ARP is the recipient of a FPU Fellowship (Spanish Ministry of Education).

Conflict of interest The authors have declared no conflict of interest.

References

Agostinelli E, Arancia G, Vedova LD, Belli F, Marra M, Salvi M, Toninello A (2004) The biological functions of polyamine oxidation products by amine oxidases: perspectives of clinical applications. Amino Acids 27:347–358

Agostinelli E, Marques MPM, Calheiros R, Gil FPSC, Tempera G, Viceconte N, Battaglia V, Grancara S, Toninello A (2010) Polyamines: fundamental characters in chemistry and biology. Amino Acids 38:393–403

Andrianantoandro E, Basu S, Karig DK, Weiss R (2006) Synthetic biology: new engineering rules for an emerging discipline. Mol Syst Biol 2:2006.0028

Auvinen M, Paasinen A, Andersson LC, Hölttä E (1992) Ornithine decarboxylase activity is critical for cell transformation. Nature 360:355–358

Berntsson PS, Alm K, Oredsson SM (1999) Half-lives of ornithine decarboxylase and S-adenosylmethionine decarboxylase activities during the cell cycle of Chinese hamster ovary cells. Biochem Biophys Res Commun 263:13–16

Cai J, Mao Z, Hwang JJ, Lu SC (1998) Differential expression of methionine adenosyltransferase genes influences the rate of growth of human hepatocellular carcinoma cells. Cancer Res 58:1444–1450

Chandrasekaran S, Price ND (2010) Probabilistic integrative modeling of genome-scale metabolic and regulatory networks in *Escherichia coli* and *Mycobacterium tuberculosis*. Proc Natl Acad Sci USA 107:17845–17850

Chaves P, Correa-Fiz F, Melgarejo E, Urdiales JL, Medina MA, Sánchez-Jiménez F (2007) Development of an expression macroarray for amine metabolism-related genes. Amino Acids 33:519–523

Corrales FJ, Pérez-Mato I, Sánchez del Pino MM, Ruiz F, Castro C, García-Trevijano ER, Latasa U, Martínez-Chantar ML, Martínez-Cruz A, Avila MA, Mato JM (2002) Regulation of mammalian liver methionine adenosyltransferase. J Nutr 132:2377S–2381S

Curien G, Bastien O, Robert-Genthon M, Cornish-Bowden A, Cárdenas ML, Dumas R (2009) Understanding the regulation of aspartate metabolism using a model based on measured kinetic parameters. Mol Syst Biol 5:271

Duarte NC, Becker SA, Jamshidi N, Thiele I, Mo ML, Vo TD, Srivas R, Palsson BØ (2007) Global reconstruction of the human metabolic network based on genomic and bibliomic data. Proc Natl Acad Sci USA 104:1777–1782

Finkelstein JD, Martin JJ (1984) Inactivation of betaine-homocysteine methyltransferase by adenosylmethionine and adenosylethionine. Biochem Biophys Res Commun 118:14–19

Finkelstein JD, Kyle WE, Martin JL, Pick AM (1975) Activation of cystathionine synthase by adenosylmethionine and adenosylethionine. Biochem Biophys Res Commun 66:81–87

Gil B, Casado M, Pajares MA, Boscá L, Mato JM, Martín-Sanz P, Alvarez L (1996) Differential expression pattern of S-adenosylmethionine synthetase isoenzymes during rat liver development. Hepatology 24:876–881

Grillo MA, Colombatto S (2008) S-adenosylmethionine and its products. Amino Acids 34:187–193

Hartwell LH, Hopfield JJ, Leibler S, Murray AW (1999) From molecular to modular cell biology. Nature 402:C47–C52

Holme P (2011) Metabolic robustness and network modularity: a model study. PLoS ONE 6:e16605

Huang ZZ, Mao Z, Cai J, Lu SC (1998) Changes in methionine adenosyltransferase during liver regeneration in the rat. Am J Physiol 275:G14–G21

Huang ZZ, Chen C, Zeng Z, Yang H, Oh J, Chen L, Lu SC (2001) Mechanism and significance of increased glutathione level in human hepatocellular carcinoma and liver regeneration. FASEB J 15:19–21

Hucka M, Finney A, Sauro HM, Bolouri H, Doyle JC, Kitano H, Arkin AP, Bornstein BJ, Bray D, Cornish-Bowden A, Cuellar AA, Dronov S, Gilles ED, Ginkel M, Gor V, Goryanin II, Hedley WJ, Hodgman TC, Hofmeyr J-H, Hunter PJ, Juty NS, Kasberger JL, Kremling A, Kummer U, Le Novère N, Loew LM, Lucio D, Mendes P, Minch E, Mjolsness ED, Nakayama Y, Nelson MR, Nielsen PF, Sakurada T, Schaff JC, Shapiro BE, Shimizu TS, Spence HD, Stelling J, Takahashi K, Tomita M, Wagner J, Wang J, Forum S (2003) The systems biology markup language (SBML): a medium for representation and exchange of biochemical network models. Bioinformatics 19:524–531

Jamshidi N, Palsson BØ (2008) Formulating genome-scale kinetic models in the post-genome era. Mol Syst Biol 4:171

Jell J, Merali S, Hensen ML, Mazurchuk R, Spernyak JA, Diegelman P, Kisiel ND, Barrero C, Deeb KK, Alhonen L, Patel MS, Porter CW (2007) Genetically altered expression of spermidine/spermine *N*1-acetyltransferase affects fat metabolism in mice via acetyl-CoA. J Biol Chem 282:8404–8413

Kee K, Foster BA, Merali S, Kramer DL, Hensen ML, Diegelman P, Kisiel N, Vujcic S, Mazurchuk RV, Porter CW (2004) Activated polyamine catabolism depletes acetyl-CoA pools and suppresses prostate tumor growth in TRAMP mice. J Biol Chem 279:40076–40083

Korendyaseva TK, Kuvatov DN, Volkov VA, Martinov MV, Vitvitsky VM, Banerjee R, Ataullakhanov FI (2008) An allosteric mechanism for switching between parallel tracks in mammalian sulfur metabolism. PLoS Comput Biol 4:e1000076

Korhonen VP, Niiranen K, Halmekytö M, Pietilä M, Diegelman P, Parkkinen JJ, Eloranta T, Porter CW, Alhonen L, Jänne J (2001) Spermine deficiency resulting from targeted disruption of the spermine synthase gene in embryonic stem cells leads to enhanced sensitivity to antiproliferative drugs. Mol Pharmacol 59:231–238

Kotb M, Mudd SH, Mato JM, Geller AM, Kredich NM, Chou JY, Cantoni GL (1997) Consensus nomenclature for the mammalian methionine adenosyltransferase genes and gene products. Trends Genet 13:51–52

Kramer DL, Sufrin JR, Porter CW (1987) Relative effects of S-adenosylmethionine depletion on nucleic acid methylation and polyamine biosynthesis. Biochem J 247:259–265

Kramer DL, Sufrin JR, Porter CW (1988) Modulation of polyamine-biosynthetic activity by S-adenosylmethionine depletion. Biochem J 249:581–586

Kramer DL, Diegelman P, Jell J, Vujcic S, Merali S, Porter CW (2008) Polyamine acetylation modulates polyamine metabolic flux, a prelude to broader metabolic consequences. J Biol Chem 283:4241–4251

Kubo S, Tamori A, Nishiguchi S, Kinoshita H, Hirohashi K, Kuroki T, Omura T, Otani S (1998) Effect of alcohol abuse on polyamine metabolism in hepatocellular carcinoma and noncancerous hepatic tissue. Surgery 123:205–211

Latasa MU, Boukaba A, García-Trevijano ER, Torres L, Rodríguez JL, Caballería J, Lu SC, López-Rodas G, Franco L, Mato JM, Avila MA (2001) Hepatocyte growth factor induces MAT2A expression and histone acetylation in rat hepatocytes: role in liver regeneration. FASEB J 15:1248–1250

Lauffenburger DA (2000) Cell signaling pathways as control modules: complexity for simplicity? Proc Natl Acad Sci USA 97:5031–5033

Le Novère N, Hucka M, Mi H, Moodie S, Schreiber F, Sorokin A, Demir E, Wegner K, Aladjem MI, Wimalaratne SM, Bergman FT, Gauges R, Ghazal P, Kawaji H, Li L, Matsuoka Y, Villéger A, Boyd SE, Calzone L, Courtot M, Dogrusoz U, Freeman TC, Funahashi A, Ghosh S, Jouraku A, Kim S, Kolpakov F, Luna A, Sahle S, Schmidt E, Watterson S, Wu G, Goryanin I, Kell DB, Sander C, Sauro H, Snoep JL, Kohn K, Kitano H (2009) The systems biology graphical notation. Nat Biotechnol 27:735–741

Li C, Courtot M, Le Novère N, Laibe C (2010) BioModels.net Web Services, a free and integrated toolkit for computational modelling software. Briefings Bioinform 11:270–277

Lu SC (2000) S-Adenosylmethionine. Int J Biochem Cell Biol 32:391–395

Ma H, Sorokin A, Mazein A, Selkov A, Selkov E, Demin O, Goryanin I (2007) The Edinburgh human metabolic network reconstruction and its functional analysis. Mol Syst Biol 3:135

Marques MPM, Gil FPSC, Calheiros R, Battaglia V, Brunati AM, Agostinelli E, Toninello A (2008) Biological activity of

antitumoural MGBG: the structural variable. Amino Acids 34:555–564

Martínez-Chantar ML, García-Trevijano ER, Latasa MU, Pérez-Mato I, Sánchez del Pino MM, Corrales FJ, Avila MA, Mato JM (2002) Importance of a deficiency in S-adenosyl-L-methionine synthesis in the pathogenesis of liver injury. Am J Clin Nutr 76:1177S–1182S

Martínez-Chantar ML, Latasa MU, Varela-Rey M, Lu SC, García-Trevijano ER, Mato JM, Avila MA (2003) L-methionine availability regulates expression of the methionine adenosyltransferase 2A gene in human hepatocarcinoma cells: role of S-adenosylmethionine. J Biol Chem 278:19885–19890

Martinov MV, Vitvitsky VM, Mosharov EV, Banerjee R, Ataullakhanov FI (2000) A substrate switch: a new mode of regulation in the methionine metabolic pathway. J Theor Biol 204:521–532

Martinov MV, Vitvitsky VM, Banerjee R, Ataullakhanov FI (2010) The logic of the hepatic methionine metabolic cycle. Biochim Biophys Acta 1804:89–96

Mato JM, Corrales FJ, Lu SC, Avila MA (2002) S-Adenosylmethionine: a control switch that regulates liver function. FASEB J 16:15–26

Medina MA, Urdiales JL, Rodríguez-Caso C, Ramírez FJ, Sánchez-Jiménez F (2003) Biogenic amines and polyamines: similar biochemistry for different physiological missions and biomedical applications. Crit Rev Biochem Mol Biol 38:23–59

Medina MA, Correa-Fiz F, Rodríguez-Caso C, Sánchez-Jiménez F (2005) A comprehensive view of polyamine and histamine metabolism to the light of new technologies. J Cell Mol Med 9:854–864

Melgarejo E, Urdiales JL, Sánchez-Jiménez F, Medina MA (2010) Targeting polyamines and biogenic amines by green tea epigallocatechin-3-gallate. Amino Acids 38:519–523

Mendes P, Hoops S, Sahle S, Gauges R, Dada J, Kummer U (2009) Computational modeling of biochemical networks using COPASI. Methods Mol Biol 500:17–59

Mikol YB, Poirier LA (1981) An inverse correlation between hepatic ornithine decarboxylase and S-adenosylmethionine in rats. Cancer Lett 13:195–201

Montañez R, Sánchez-Jiménez F, Aldana-Montes JF, Medina MA (2007) Polyamines: metabolism to systems biology and beyond. Amino Acids 33:283–289

Montañez R, Rodríguez-Caso C, Sánchez-Jiménez F, Medina MA (2008) In silico analysis of arginine catabolism as a source of nitric oxide or polyamines in endothelial cells. Amino Acids 34:223–229

Montañez R, Medina MA, Solé RV, Rodríguez-Caso C (2010) When metabolism meets topology: reconciling metabolite and reaction networks. Bioessays 32:246–256

Newman MEJ (2006) Modularity and community structure in networks. Proc Natl Acad Sci USA 103:8577–8582

Nijhout HF, Reed MC, Budu P, Ulrich CM (2004) A mathematical model of the folate cycle: new insights into folate homeostasis. J Biol Chem 279:55008–55016

Nijhout HF, Reed MC, Lam S-L, Shane B, Gregory JF, Ulrich CM (2006) In silico experimentation with a model of hepatic mitochondrial folate metabolism. Theor Biol Med Model 3:40

Parry L, Balaña Fouce R, Pegg AE (1995) Post-transcriptional regulation of the content of spermidine/spermine *N*1-acetyltransferase by *N*1*N*12-bis(ethyl)spermine. Biochem J 305(Pt 2):451–458

Paz JC, Sánchez-Jiménez F, Medina MA (2001) Characterization of spermine uptake by Ehrlich tumour cells in culture. Amino Acids 21:271–279

Pezzato E, Battaglia V, Brunati AM, Agostinelli E, Toninello A (2009) Ca^{2+} -independent effects of spermine on pyruvate dehydrogenase complex activity in energized rat liver mitochondria incubated in the absence of exogenous Ca^{2+} and Mg^{2+}. Amino Acids 36:449–456

Prudova A, Martinov MV, Vitvitsky VM, Ataullakhanov FI, Banerjee R (2005) Analysis of pathological defects in methionine metabolism using a simple mathematical model. Biochim Biophys Acta 1741:331–338

Prudova A, Bauman Z, Braun A, Vitvitsky VM, Lu SC, Banerjee R (2006) S-adenosylmethionine stabilizes cystathionine beta-synthase and modulates redox capacity. Proc Natl Acad Sci USA 103:6489–6494

Raftos JE, Whillier S, Kuchel PW (2010) Glutathione synthesis and turnover in the human erythrocyte: alignment of a model based on detailed enzyme kinetics with experimental data. J Biol Chem 285:23557–23567

Rao CV, Arkin AP (2001) Control motifs for intracellular regulatory networks. Annu Rev Biomed Eng 3:391–419

Reed MC, Nijhout HF, Sparks R, Ulrich CM (2004) A mathematical model of the methionine cycle. J Theor Biol 226:33–43

Reed MC, Thomas RL, Pavisic J, James SJ, Ulrich CM, Nijhout HF (2008) A mathematical model of glutathione metabolism. Theor Biol Med Model 5:8

Reyes-Palomares A, Montañez R, Real-Chicharro A, Chniber O, Kerzazi A, Navas-Delgado I, Medina MA, Aldana-Montes JF, Sanchez-Jimenez F (2009) Systems biology metabolic modeling assistant: an ontology-based tool for the integration of metabolic data in kinetic modeling. Bioinformatics 25:834–835

Rodríguez-Caso C, Montañez R, Cascante M, Sánchez-Jiménez F, Medina MA (2006) Mathematical modeling of polyamine metabolism in mammals. J Biol Chem 281:21799–21812

Russell DH, McVicker TA (1971) Polyamine metabolism in mouse liver after partial hepatectomy. Biochim Biophys Acta 244:85–93

Sánchez del Pino MM, Pérez-Mato I, Sanz JM, Mato JM, Corrales FJ (2002) Folding of dimeric methionine adenosyltransferase III: identification of two folding intermediates. J Biol Chem 277:12061–12066

Sánchez-Jiménez F, Montañez R, Correa-Fiz F, Chaves P, Rodríguez-Caso C, Urdiales JL, Aldana JF, Medina MA (2007) The usefulness of post-genomics tools for characterization of the amine cross-talk in mammalian cells. Biochem Soc Trans 35:381–385

Santamaría E, Muñoz J, Fernandez-Irigoyen J, Sesma L, Mora MI, Berasain C, Lu SC, Mato JM, Prieto J, Avila MA, Corrales FJ (2006) Molecular profiling of hepatocellular carcinoma in mice with a chronic deficiency of hepatic s-adenosylmethionine: relevance in human liver diseases. J Proteome Res 5:944–953

Shen-Orr SS, Milo R, Mangan S, Alon U (2002) Network motifs in the transcriptional regulation network of *Escherichia coli*. Nat Genet 31:64–68

Smallbone K, Simeonidis E, Swainston N, Mendes P (2010) Towards a genome-scale kinetic model of cellular metabolism. BMC Syst Biol 4:6

Snoep JL, Bruggeman F, Olivier BG, Westerhoff HV (2006) Towards building the silicon cell: a modular approach. BioSystems 83:207–216

Stipanuk MH, Dominy JE (2006) Surprising insights that aren't so surprising in the modeling of sulfur amino acid metabolism. Amino Acids 30:251–256

Sullivan DM, Hoffman JL (1983) Fractionation and kinetic properties of rat liver and kidney methionine adenosyltransferase isozymes. Biochemistry 22:1636–1641

Vitvitsky V, Mosharov E, Tritt M, Ataullakhanov F, Banerjee R (2003) Redox regulation of homocysteine-dependent glutathione synthesis. Redox Rep 8:57–63

Vitvitsky V, Thomas M, Ghorpade A, Gendelman HE, Banerjee R (2006) A functional transsulfuration pathway in the brain links to glutathione homeostasis. J Biol Chem 281:35785–35793

Williams-Ashman HG, Coppoc GL, Weber G (1972) Imbalance in ornithine metabolism in hepatomas of different growth rates as expressed in formation of putrescine, spermidine, and spermine. Cancer Res 32:1924–1932